Centrality and transverse momentum dependence of hadrons in Au+Au collisions at BES energy region

Huanjing Gong,[1] Zhizhen Ye,[1] Guiqi Liu,[1] and Lilin Zhu[*]

[1] *Department of Physics, Sichuan University, Chengdu 610064, China*

The transverse momentum spectra of seven identified hadrons (π, K, p, Λ, ϕ, Ξ, Ω) produced in Au+Au collisions in the BES energy region have been investigated in the framework of the recombination model (RM). The investigation has testified that the results are extended successfully to the p_T distributions in the energy range of Beam-Energy Scan (BES) Program at the Relativistic Heavy-Ion Collider (RHIC) over wide ranges of p_T, particularly in the region of low p_T. Our study shows great agreement between theoretical results and experimental data with only two parameters. With all of dependence taken into account, the exciting results shows good similarity of final state hardons in quite a wide collision energy from $\sqrt{s_{NN}} = 7.7$ GeV to $\sqrt{s_{NN}} = 5.02$ TeV. Besides, valon model is expected to apply to K production in Au+Au collisions and our attempt is exhibited in the followings.

PACS numbers: 25.75.Nq, 25.75.Ld

I. INTRODUCTION

Quark gluon plasma (QGP) is the main state of universe in the earlier period after big bang, which makes a big difference on the evolution of cosmos. Strongly interacting matter composed of hadronic constituents, like proton and neutron, undergoes the phase transition to QGP in a high-energy-density and high-temperature phase where the quantum chromodynamics (QCD) phase diagram exhibits in high-energy heavy-ion collision experiments. Experimentally, the final state observables is the crucial tools as figuring out the mechanism of recombination of particles. Hwa-Yang recombination model is adopted to describe the universal productions for all identified hadrons over wide ranges of transverse momenta in heavy-ion collisions pretty well[2]. Moreover, in order to map out the phase diagram of the QCD matter, a Beam Energy Scan (BES) program has been initiated at RHIC with Au+Au collisions at $\sqrt{s_{NN}} = 7.7 \sim 39$ GeV [1]. In this paper, seven identified hadrons (π, K, p, Λ, ϕ, Ξ, Ω) are included to expand our investigation in beam energy region at $\sqrt{s_{NN}} = 7.7 \sim 39$ GeV and centrality has been taken into account.

In Section II, we will introduce the formulation of recombination to calculate the p_T distribution, which mainly include thermal and shower partons. The exponential behavior of thermal partons is valid over wide ranges of p_T while show parton distribution is integrated over jet momentum and summed over all jets. In the BES region, the momentum of quarks is much lower than in the intermediate region, resulting in the dominant $\mathcal{TT}$ and $\mathcal{TTT}$ components and the negligible components associated with $\mathcal{S}$. Therefore, we show the huge difference in several orders of magnitude in Section II and then in Section IV we only consider the $\mathcal{TT}$ and $\mathcal{TTT}$ components that play the dominant role in fact.

In Section III, we follow up the notion in [4] to consider a baryon spectra to obtain two coefficients which can be calculated in [3] by linearly fitting the experimental data of spectra. And in Section IV, we will give the formulation of transition between baryon spectra and p_T distribution of hadrons to derive the significant parameter normalization C_j and inverse slope T_j. Subsequently, in Section V we display the results from our study on the centrality dependence of transverse momentum spectra of seven identified hadrons in Au+Au collisions at $\sqrt{s_{NN}} = 7.7 \sim 39$ GeV.

Besides, we have studied hadronic collisions in the valon-recombination model (VRM) [5], which is expected to fix the slight deviation in Section II for kaon. In Section VI, valon model is presented to calculate proton inclusive distributions with two parameters. What's new is that we adopt a rough approximation that one of the two baryons in hadronic collisions can be simply regarded as the combination of protons and neutrons so that particle production in AA collisions can be calculated, while the processes, not only of pp, but also of pA collisions have been checked with valon-recombination model [6]. Finally, section VII summarizes the results and makes a conclusion in terms of the present work, as well as the expectation of implementation of valon model in Au+Au collisions.

II. FORMULATION OF QUARK RECOMBINATION

As recombination model mentioned [2–5], we start from the universal formalism in brief to calculate the p_T distribution. The basic framework by definition emphasizes that thermal and shower partons in jets or minijets at midrapidity undergo the processes of recombination, resulting in the production of mesons and baryons. Therefore, the formula of distributions naturally is a convolution of the parton distribution with the recombina-

*Electronic address: zhulilin@scu.edu.cn

tion function over η at midrapidity

$$p^0\frac{dN^M}{dp_T} = \int \frac{dp_1}{p_1}\frac{dp_2}{p_2}F_{q_1\bar{q}_2}(p_1,p_2)R^M_{q_1\bar{q}_2}(p_1,p_2,p_T), \quad (1)$$

$$p^0\frac{dN^B}{dp_T} = \int \frac{dp_1}{p_1}\frac{dp_2}{p_2}\frac{dp_3}{p_3}F_{q_1q_2q_3}(p_1,p_2,p_3) \times R^B_{q_1q_2q_3}(p_1,p_2,p_3,p_T), \quad (2)$$

in which q_i means the transverse momenta of quarks and R^M and R^B represents the recombination functions for mesons and baryons. Then, the paton distributions are partitioned into several components

$$F_{q_1\bar{q}_2} = \mathcal{TT} + \mathcal{TS} + \mathcal{SS}, \quad (3)$$

$$F_{q_1q_2q_3} = \mathcal{TTT} + \mathcal{TTS} + \mathcal{TSS} + \mathcal{SSS}, \quad (4)$$

where $\mathcal{T}$ and $\mathcal{S}$ represent the invariant distributions for thermal and shower partons in terms of momenta just before hadronization, respectively. At BES energy region, as seen later, $\mathcal{S}$ components are small enough to neglect while the dominant $\mathcal{TT}$ and $\mathcal{TTT}$ components are mainly calculated, owing to the low transverse momenta p_i caused by the low energy of the colliding system.

A simple exponential form is assumed statistically for the thermal parton distribution

$$\mathcal{T}_j(p_i) = p_i\frac{dN_j}{dp_i} = C_j p_i e^{-p_i/T_j}, \quad (5)$$

where the subscript j denotes quark (u,d,s). Since the mass of s is different from (u,d), to distinguish them, we use q to denote (u,d). The normalization factor C_j, dependent of the number of participants N_{part} and $\sqrt{s_{NN}}$, has the dimension of inverse momentum and the inverse slope T_j, only dependent of $\sqrt{s_{NN}}$, is determined by fitting the experimental data of spectra at low p_T[3] and includes the dissipative effects of minijets on the expanding medium at all times of the evolution of the plasma[4]. Furthermore, we use the universal formula for the energy dependence of T_j in [4],

$$T_q(s) = T_1 f(s), \qquad T_s(s) = T_2 f(s), \quad (6)$$

$$f(s) = \sqrt{s}^{\,\beta}, \qquad \sqrt{s} \text{ in TeV} \quad (7)$$

with the slightly different in [4] but same in [2] parameters

$$T_1 = 0.39 \text{ GeV/c}, \quad T_2 = 0.51 \text{ GeV/c}, \quad \beta = 0.105. \quad (8)$$

Hereafter, $\sqrt{s}$ in the formulae denotes $\sqrt{s_{NN}}$. The values of T_j are given in Table I.

Now, we just give the formula of the shower parton distribution, associated with the fragmentation function and distribution of jet, and more details have been explicated in [2] because component $\mathcal{S}$ is not needed and interested at BES region.

$$\mathcal{S}^j(p_2,c) = \int \frac{dq}{q}\sum_i \hat{F}_i(q,c)S_i^j(p_2,q). \quad (9)$$

$\sqrt{s}$ (GeV)	7.7	11.5	19.6	27	39
T_q (GeV)	0.234	0.244	0.258	0.267	0.277
T_s (GeV)	0.306	0.319	0.338	0.349	0.363

TABLE I: Parameters T_q and T_s for Au+Au collisions at $\sqrt{s} = 7.7, 11.5, 19.6, 27$ and 39 GeV, respectively.

Fig.1 shows the transverse momentum spectra for seven identified hadrons (π, K, p, Λ, ϕ, Ξ, Ω) in Au+Au collisions at $\sqrt{s_{NN}} = 39$ GeV and the collision of 0-5%. According to the p_T spectra, $\mathcal{TT}$ and $\mathcal{TTT}$ components are seen to be absolutely dominant so the effects of minijets and jets can be ignored, whereupon in Secs. III and IV we only talk over the dominant components. And another thing worthy of attention is that the theoretical curves fit remarkably the experimental data by two parameters C and C_s given below except for the kaon distribution.

$$C_q = 38.0, \quad C_s = 10.7. \quad (10)$$

Hence, we attempt to utilize the valon-recombination model(VRM) to improve the transverse momentum distribution of K produced in Au-Au collision in Section VI.

To correspond to the following section, a simplified parton distribution should be gained, which specifically presented in Section IV. Now we can write the recombination function as

$$R_h(p_1,p_2,p_3,p_T) = W_h(y_1,y_2,y_3)\delta\Big(\sum_i y_i - 1\Big), \quad (11)$$

where $y_i = p_i/p_T$, which is the momentum fraction of the ith quark in the hadron h, and for proton $W_p(y_1,y_2,y_3)$ has been studied in the valon model[9] discussed in Section VI. Then there follows the condition for baryons and the figure for mesons also follow the notion. On the basis that the average momentum fraction y_i of each quark in a hyperon is 1/3, we simplify Eq.11 further by the approximation for all h[4],

$$R_h(p_1,p_2,p_3,p_T) = \mathrm{g}_h\prod_{i=1}^{3}\delta(p_i/p_T - 1/3), \quad (12)$$

where g_h is a numerical factor depends only on hadron. Substituting Eqs.4,5 and 12 into Eq.2, the universal baryon distribution is

$$p^0\frac{d\bar{N}}{dp_T} = \Big(\prod_{i=1}^{3}C_i\Big)g_h p_T^3\exp\Big[-\frac{p_T}{T_h}\Big], \quad (13)$$

where T_h satisfies the following identification:

$$T_h = \frac{1}{3}\sum_i\frac{1}{T_i} = \frac{1}{3}\Big(\frac{3-n_s}{T_q} + \frac{n_s}{T_s}\Big), \quad (14)$$

where n_s is the number of strange quarks in h. At midrapidity considered here and in [2], we have $p^0 \approx m_T^h$, where $m_T^h = (m_h^2 + p_T^2)^{1/2}$, m_h being the mass of baryon h.

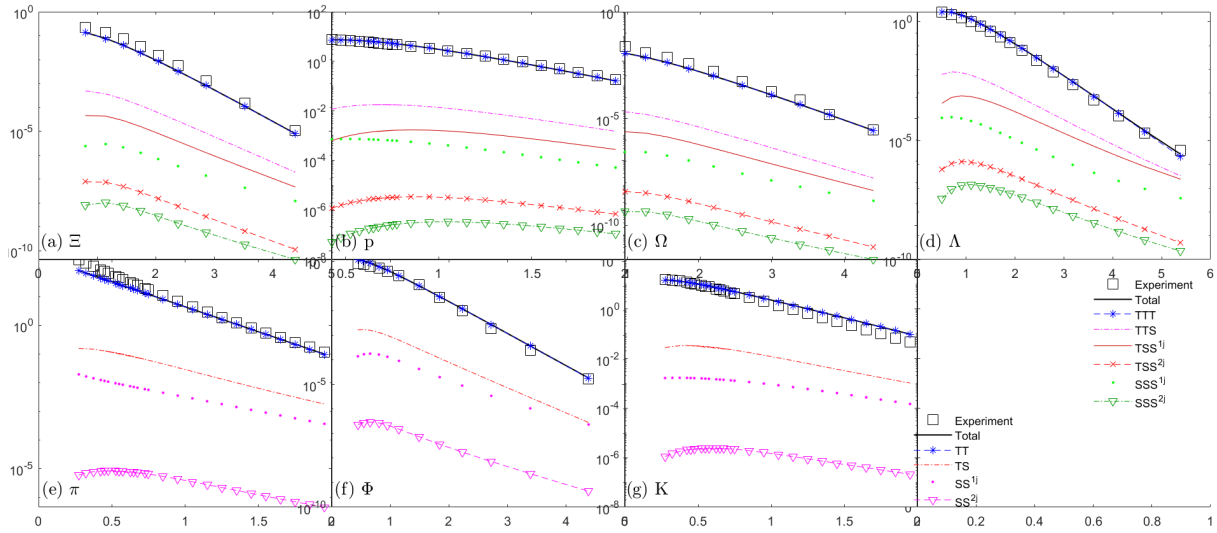

FIG. 1: Transverse momentum spectra of Ξ (a), proton (b), Ω (c), Λ (d), π (e), ϕ (f) and K (g) from the recombination model at midrapidity for Au+Au collisions at $\sqrt{s_{NN}} = 39$ GeV and centralities of 0-5%. The experimental data are taken from Ref. [1, 7, 8].

III. BARYON AND MESON SPECTRA

With the results above, we consider to stay close to the data and search for a description that is applicable to all baryons and mesons to obtain the universal formalism and parameters[4]. Firstly, we transform the p_T spectra to linear formula for baryons and mesons respectively

$$B_h(s, N_{part}, p_T) = \frac{m_T^h}{p_T^2} \frac{d\bar{N}_h}{p_T dp_T}(s, N_{part}), \quad (15)$$

$$M_h(s, N_{part}, p_T) = \frac{m_T^h}{p_T} \frac{d\bar{N}_h}{p_T dp_T}(s, N_{part}), \quad (16)$$

Note that B_h has dimension$(momentum)^{-3}$ and M_h has dimension$(momentum)^{-2}$. In Figs.4∼8, we show the B_h or M_h spectra from Au+Au collisions at $\sqrt{s}$=7.7, 11.5, 19.6, 27, 39 GeV for five hadrons and different centrality classes. The straight-line fits pretty well so we can define the phenomenological formula to describe the exponential dependence on p_T for all hadrons at BES region

$$B_h(s, N_{part}, p_T) = A_h(s, N_{part})\exp[-p_T/T_h(s)], \quad (17)$$
$$M_h(s, N_{part}, p_T) = A_h(s, N_{part})\exp[-p_T/T_h(s)], \quad (18)$$

We can determine from the heights of the straight lines in Figs.4∼8 the prefactors of the exponentials, which turn out to behave simply as[4]

$$A_h(s, Npart) = A_h^1(s) N_{part}^{a_h}, \quad (19)$$

in which a_h=1.35 for all baryons and a_h=0.9 for ϕ. Fig.2 shows the results for four baryons at BES energies. And the coefficient A_h^1(s) have the power-law behavior, shown in Fig.3.

	A_h^0	b_h
p	0.0052	0.877
Λ	0.0088	0.444
Ξ	0.0023	0.100
Ω	1.7635×10^{-4}	0.050

TABLE II: Values of A_h^0 and b_h in Eq.20.

$$A_h^1(s) = A_h^0 \sqrt{s}^{-b_h}, \qquad \sqrt{s} \text{ in TeV} \quad (20)$$

where the values of A_h^0 and b_h are given in Table II.

Looking back to Eq.15 and Eq.16, compared with Eq.17 and Eq.18, C_q and C_s are determined by the following equations

$$A_\phi(s, N_{part}) = g_\phi C_s^2(s, N_{part}), \quad (21)$$
$$A_p(s, N_{part}) = g_{st}^p g_p g_p' C_q^3(s, N_{part}), \quad (22)$$

which will be discussed in the next section.

IV. TRANSVERSE MOMENTUM DISTRIBUTION OF HADRONS

As stated above, the two essential coefficient C_q and C_s, which corresponds to (u,d) quark and s quark respectively, can be obtained from baryon spectra function of proton (B_p) and meson spectra function of ϕ (M_ϕ).

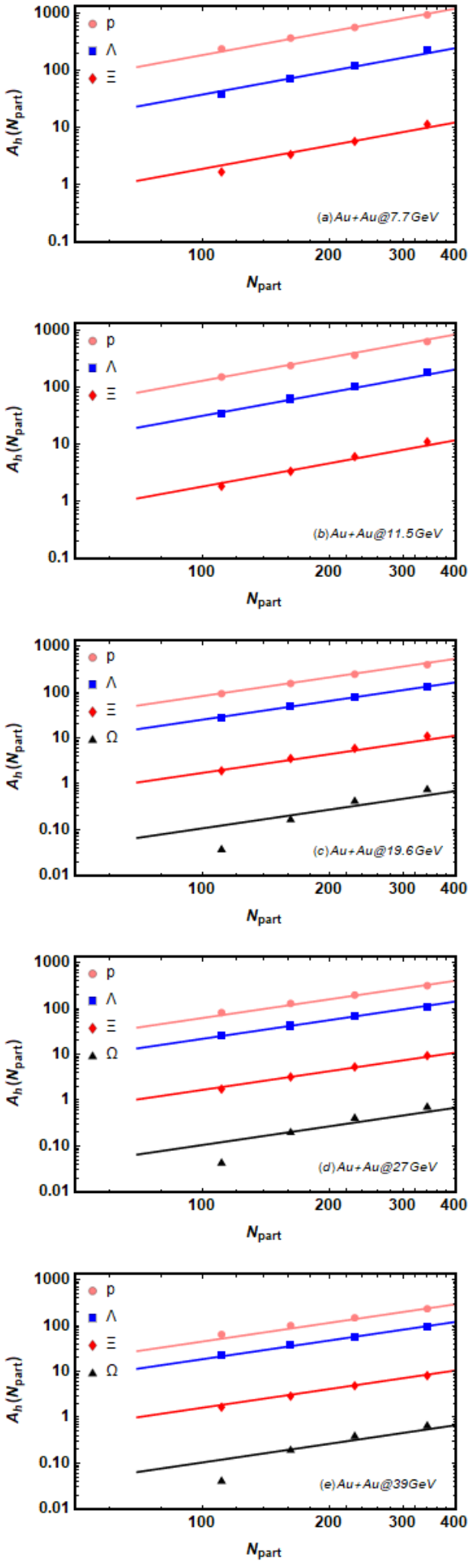

FIG. 2: A_h vs N_{part} for five colliding energies.

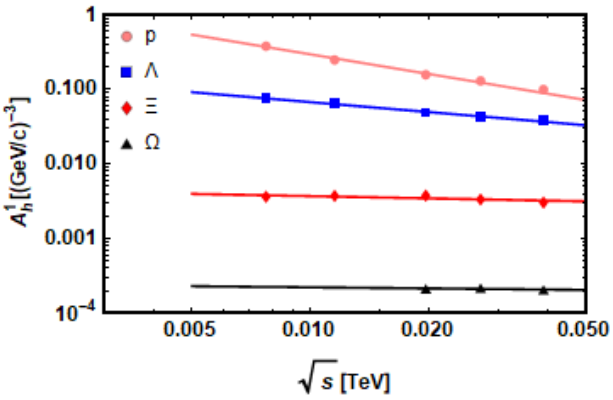

FIG. 3: A_h^1(s) vs $\sqrt{s}$ for the four baryons. The lines are fits of the solid points by Eq.20 with values of A_h^0 and b_h in Table II.

After the recombination functions(RM) of all the identified hadrons are derived, we summarize the transverse momentum distributions of them explicitly here.

A. Proton production

The RM for proton is given in Refs.[2, 10–13], and thus the thermal-thermal-thermal(TTT) recombination is

$$\frac{dN_p^{TTT}}{p_T dp_T} = g_{st}^p g_p g_p' \frac{C_q^3 p_T^2}{m_T^p} e^{-p_T/T_q}, \tag{23}$$

where $g_{st}^p = 1/6$ and

$$g_p = [B(\alpha+1, \alpha+\beta+2)B(\alpha+1, \beta+1)]^{-1}, \tag{24}$$

$$g_p' = B(\alpha+2, \beta+2)B(\alpha+2, \alpha+\beta+4). \tag{25}$$

$B(\alpha, \beta)$ is the beta function with $\alpha = 1.75$ and $\beta = 1.05$. Afterwards, compared with Eq.17, we multiply Eq.23 by m_T^p/p_T^2 to derive C_q shown in Table III from Eq.22

$$C_q(s, N_{part}) = [A_p(s, N_{part})/g_{st}^p g_p g_p']^{1/3}. \tag{26}$$

The value of C_q is generally consistent with it in Eq.10. After that, we figure out the transverse momentum distribution of proton by substituting C_q and T_q into Eq.23.

B. ϕ production

Then, we consider the production of ϕ. When the RF is taken to be [14]

$$R_{s\bar{s}}(p_1, p_2, p_T) = \mathrm{g}_\phi p_1 p_2 \prod_{i=1}^{2} \delta(p_i - p_T/2), \tag{27}$$

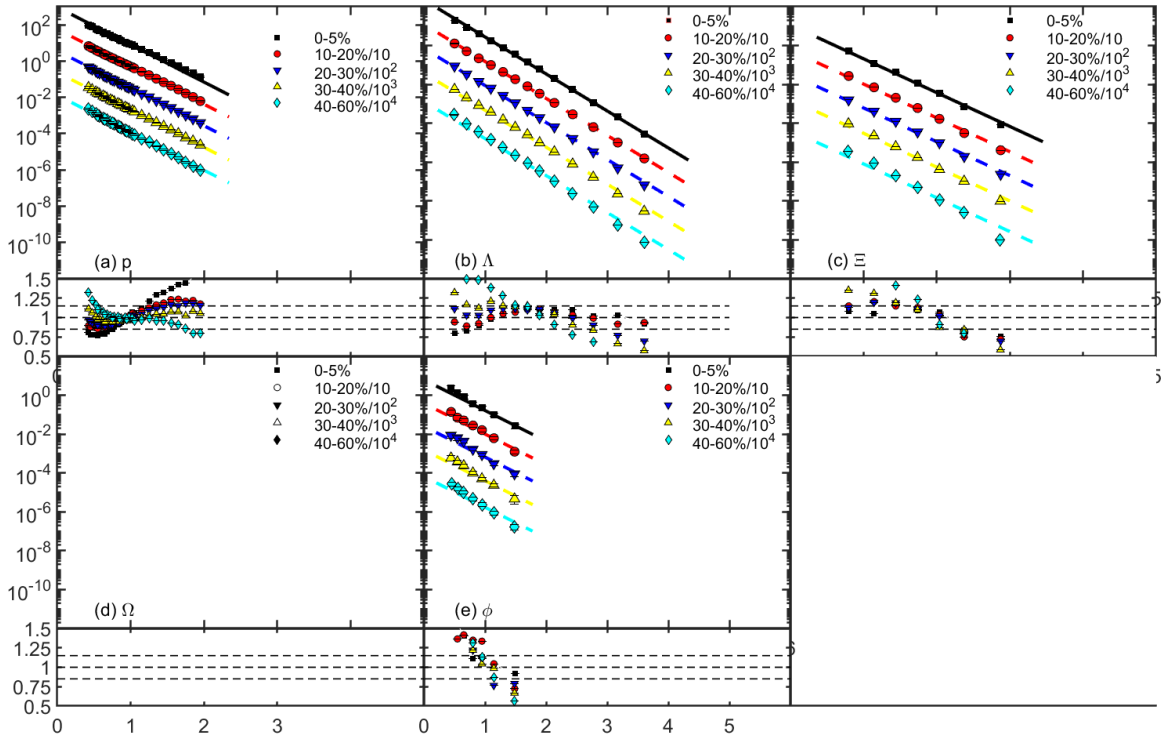

FIG. 4: (colored online)Baryon or meson spectra function ($B_h(p_T)$, $M_h(p_T)$) for proton (a), Λ (b), Ξ (c), Ω (d) and ϕ (e) for Au+Au collisions at $\sqrt{s_{NN}} = 7.7$ GeV. The experimental value/theoretical value ratios lie in the bottom of each subfigure. The experimental data are taken from Refs. [1, 7, 8].

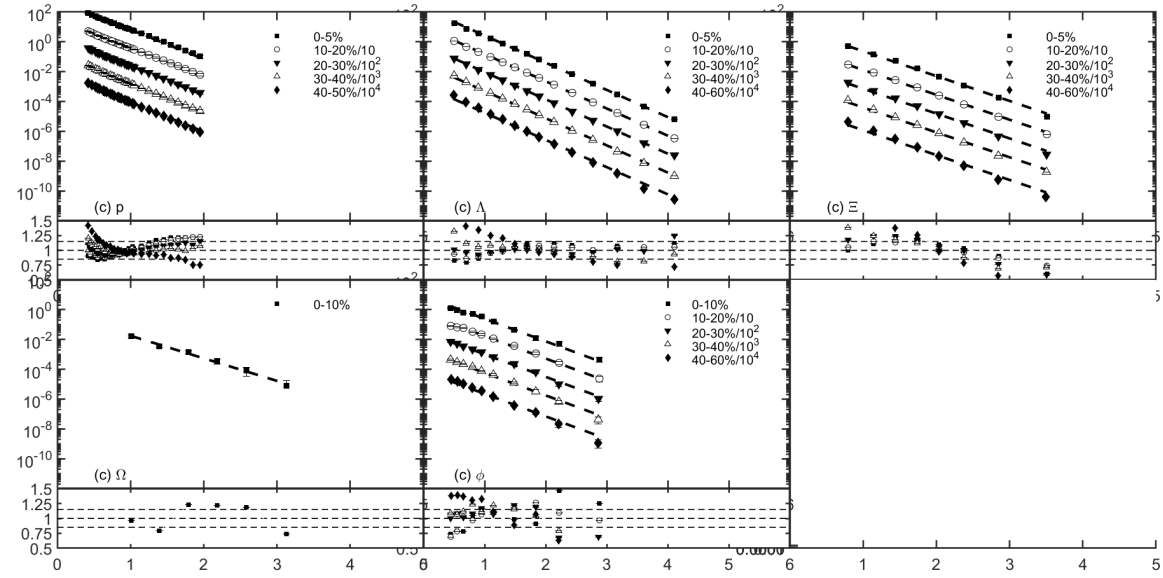

FIG. 5: (colored online)Baryon or meson spectra function ($B_h(p_T)$, $M_h(p_T)$) for proton (a), Λ (b), Ξ (c), Ω (d) and ϕ (e) for Au+Au collisions at $\sqrt{s_{NN}} = 11.5$ GeV. The experimental value/theoretical value ratios lie in the bottom of each subfigure. The experimental data are taken from Refs. [1, 7, 8].

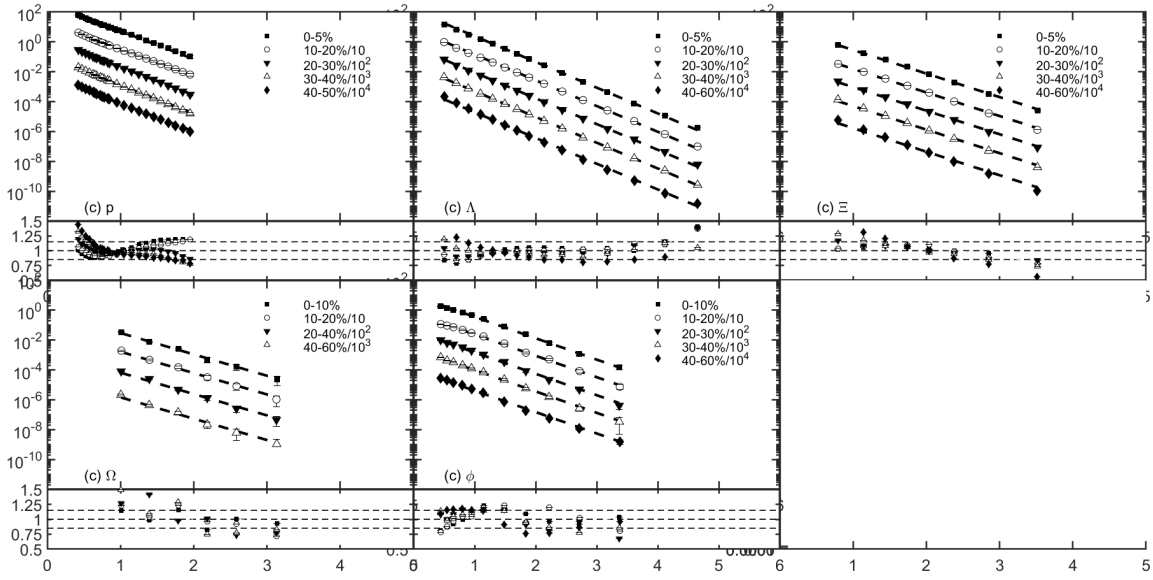

FIG. 6: (colored online)Baryon or meson spectra function ($B_h(p_T)$, $M_h(p_T)$) for proton (a), Λ (b), Ξ (c), Ω (d) and ϕ (e) for Au+Au collisions at $\sqrt{s_{NN}} = 19.6$ GeV. The experimental value/theoretical value ratios lie in the bottom of each subfigure. The experimental data are taken from Refs. [1, 7, 8].

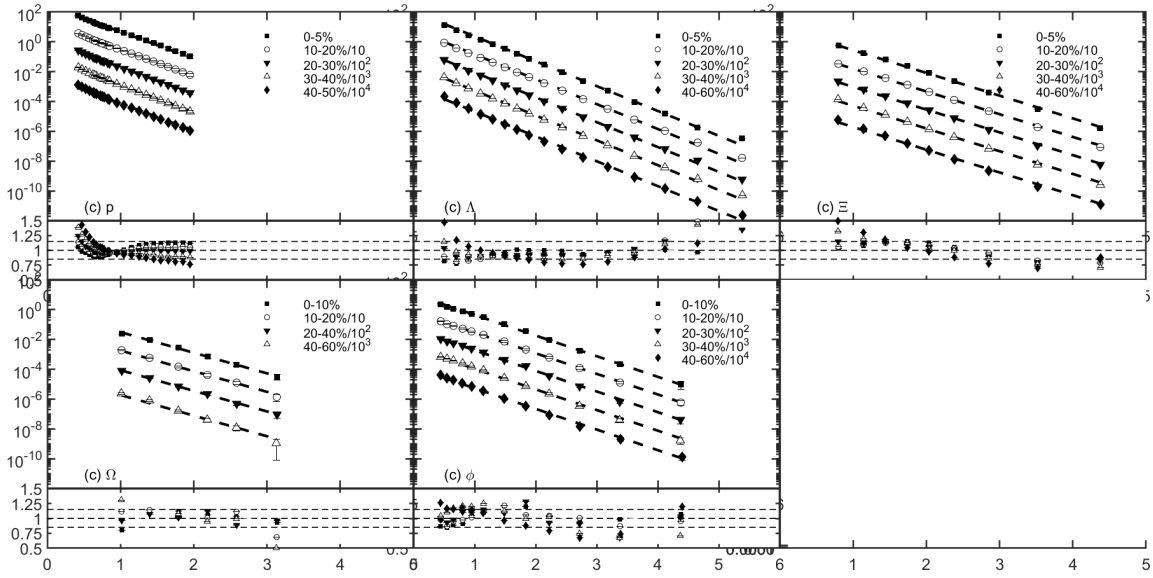

FIG. 7: (colored online)Baryon or meson spectra function ($B_h(p_T)$, $M_h(p_T)$) for proton (a), Λ (b), Ξ (c), Ω (d) and ϕ (e) for Au+Au collisions at $\sqrt{s_{NN}} = 27$ GeV. The experimental value/theoretical value ratios lie in the bottom of each subfigure. The experimental data are taken from Refs. [1, 7, 8].

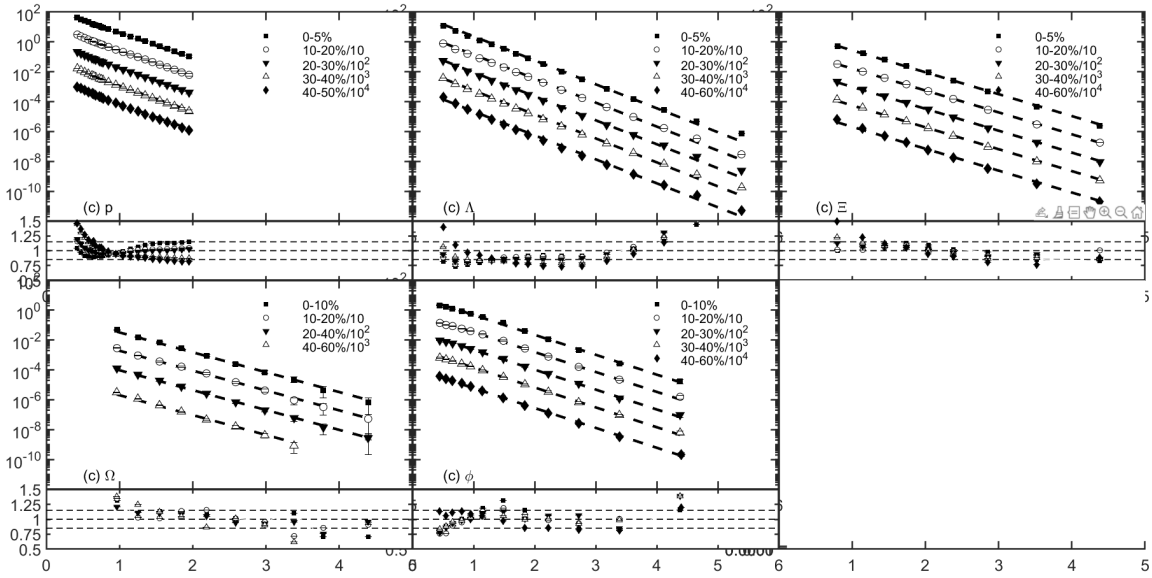

FIG. 8: Baryon or meson spectra function ($B_h(p_T)$, $M_h(p_T)$) for proton (a), Λ (b), Ξ (c), Ω (d), ϕ (e), for Au+Au collisions at $\sqrt{s_{NN}} = 39$ GeV. The experimental value/theoretical value ratios lie in the bottom of each subfigure. The experimental data are taken from Refs. [1, 7, 8].

where g_ϕ=0.432, the distribution for ϕ is gained.

$$\frac{dN_\phi^{TT}}{p_T dp_T} = g_\phi \frac{C_s^2 p_T}{4m_T^\phi} e^{-p_T/T_s}, \tag{28}$$

And similarly we multiply Eq.28 by m_T^ϕ/p_T to obtain C_s shown in Table IV from Eq.21

$$C_s(s, N_{part}) = [4A_\phi(s, N_{part})/g_\phi]^{1/2}. \tag{29}$$

Therefore, the distributions for all identified hadrons, including ϕ, can be calculated since we have the values of C_q and C_s at all centralities and energies.

C. Ξ, Λ and Ω production

The p_T distributions of Ξ, Λ and Ω are quite similar to that of proton. The differences among them are the number of strange quarks in h and the RF for various hadrons. Since the RF for Ξ, Λ and Ω have been given in [2, 13, 14], we have

$$\frac{dN_\Xi^{TTT}}{p_T dp_T} = \frac{g_\Xi C_q C_s^2 p_T^2}{27m_T^\Xi} e^{-p_T/3T_q} e^{-2p_T/3T_s}, \tag{30}$$

where g_Ξ=0.03,

$$\frac{dN_\Lambda^{TTT}}{p_T dp_T} = g_{st}^\Lambda N_\Lambda [B(\alpha+2, \beta+2)B(\alpha+2, \alpha+\beta+4)] \frac{C_q^2 C_s p_T^2}{m_T^\Lambda} e^{-2p_T/3T_q} e^{-p_T/3T_s}, \tag{31}$$

where g_{st}^Λ=1/8(1/2 for Λ^0 or Σ^0, and 2/8 from spin consideration) and the RF parameters for Λ are α=1, β=2, and

$$\frac{dN_\Omega^{TTT}}{p_T dp_T} = \frac{g_\Omega C_s^3 p_T^2}{27m_T^\Omega} e^{-p_T/T_s}, \tag{32}$$

where g_Ω=0.01.

V. RESULTS

So far, we have presented the equations of the five hadronic spectra. As for π and K, the contribution from the resonance decays must be considered, which is taken into account in Fig.1 and not interested here. For thermal partons, the inverse slopes T and T_s are independent of centrality, so the free parameters are just the centrality dependence of normalization factors, C_q and C_s[3].

The results from RM in Au+Au collisions for five identified hadrons, i.e.,p, Λ, ϕ, Ξ and Ω, are shown in Figs.9∼13. All centralities and five energies at BES region are taken into account. Data are from Refs.[1, 7, 8]. The dashed lines from calculations reproduce the p_T distributions well in general throughout the whole region where data exist. In addition, we predict the spectra of Ω in central and non-central Au+Au collisions at $\sqrt{s}$=7.7, 11.5 GeV with recombination model, which can be testified in the future.

All the experimental value/theoretical value ratios are limited within 1.5. Although the ratios do not show the perfect agreement, it is a significant achievement to get a good fit over wide ranges of p_T for all the identified hadrons at various centralities in quite a wide collision

centrality / $\sqrt{s}$(GeV)	0-5%	10-20%	20-30%	30-40%	40-60%
7.7	60.7031	51.3111	44.4750	38.4560	31.4561
11.5	53.3346	44.3816	38.6098	33.1342	27.3459
19.6	45.5197	38.8299	33.2419	28.0365	23.8158
27	42.1296	35.9997	31.3034	26.8425	22.4945
39	38.0702	32.7682	28.7857	24.8077	20.8087

TABLE III: Values of $C_q[(GeV/c)^{-1}]$ at various centralities and energies in Au+Au collision. The values of N_{part} are taken from [8].

centrality / $\sqrt{s}$(GeV)	0-5%	10-20%	20-30%	30-40%	40-60%
7.7	7.6029	5.9358	4.8195	3.7510	2.4599
11.5	8.6279	7.2180	5.5505	4.1935	2.6197
19.6	9.4689	7.7271	6.0909	4.9368	3.1813
27	9.9892	8.0698	6.5269	4.9392	3.4590
39	9.7526	8.1763	6.6462	5.3283	3.4642

TABLE IV: Values of $C_s[(GeV/c)^{-1}]$ at various centralities and energies in Au+Au collision. The values of N_{part} are taken from [8].

energy. Accordingly, it is deduced that recombination model is a excellent approach to describe the transverse momentum and centrality dependence of hadron production in the nuclear collisions.

VI. VALON-RECOMBINATION MODEL

Aiming at the slight deviation for p_T distribution of kaon in Fig.1(g), we pay attention to the valon-recombination model(VRM)[5, 9, 15–17]. In the quark model suitable for describing deep-inelastic scattering process by CTEQ[9], there are three valence quarks plus an infinity of sea quarks and gluons[17], and we shall regarded these clusters as valons. Each valon has a valence quark, as well as its own sea quarks and gluons, playing a role in the collision problem as the constituent quarks do in the bound-state problem[15]. The valon model has been studied in p-p and p-A collisions when the CTEQ data and p-Pb data in the NA49 experiment are published previously. Now we attempt to generalize VRM to A-A collisions. Firstly we need a rough assumption, in which one of the two targets is decomposed into the single valons so that we can calculate momentum distribution for proton from the available results[15] in p-A collisions.

Let us begin with the invariant distribution function for the detection of a proton at momenta fraction x is

$$H_p(x) = \frac{1}{N}\int \frac{dx_1}{x_1}\frac{dx_2}{x_2}\frac{dx_3}{x_3}F(x_1,x_2,x_3) \times R_p(x_1,x_2,x_3,x), \quad (33)$$

where N is the normalization factor. Note the two invariant distributions: $F(x_1,x_2,x_3)$ denotes the probability of finding a u quark at x_1, another u quark at x_2, and a d quark at x_3, and $R_p(x_1,x_2,x_3,x)$ denotes the recombination function, which specifies the probability that those three quarks coalesce to form a proton at x.

The quark distribution from the proton is

$$F_p(x_1,x_2,x_3) = \int dy_1' dy_2' dy_3' G_{\overline{v}}'(y_1',y_2',y_3') \times M_p(y_1',y_2',y_3';x_1,x_2,x_3), \quad (34)$$

where $G_{\overline{v}}'$ is associated with the valon distribution after momentum degradation and M_p denotes various types of recombination from quarks in valons to identified hadrons, which are all given in [15]. Similarly, we can get anti-proton distribution function $H_{\overline{p}}(x)$, after which we obtain the final formula for net proton production

$$H_{p-\overline{p}}(x) = H_p(x) - H_{\overline{p}}(x). \quad (35)$$

Following by the notion above, the momentum distribution for kaon is available.

VII. CONCLUSION

In this paper, we have studied seven identified hadron spectra in the recombination model in Au+Au collisions at beam energy region at RHIC. The theoretical results reproduce the experimental data very well at $\sqrt{s}$=7.7, 11.5, 19.6, 27, 39 GeV and all centralities. Moreover, we figure out the universal exponential features without model input by defining the baryon and meson spectra functions, and then we derive the parameters $C_j(s,N_{part})$ at BES region.

Finally, Considering the slight deviation of spectra for K, we come up with the valon-recombination model that had been studied previously. Although the VRM in A-A

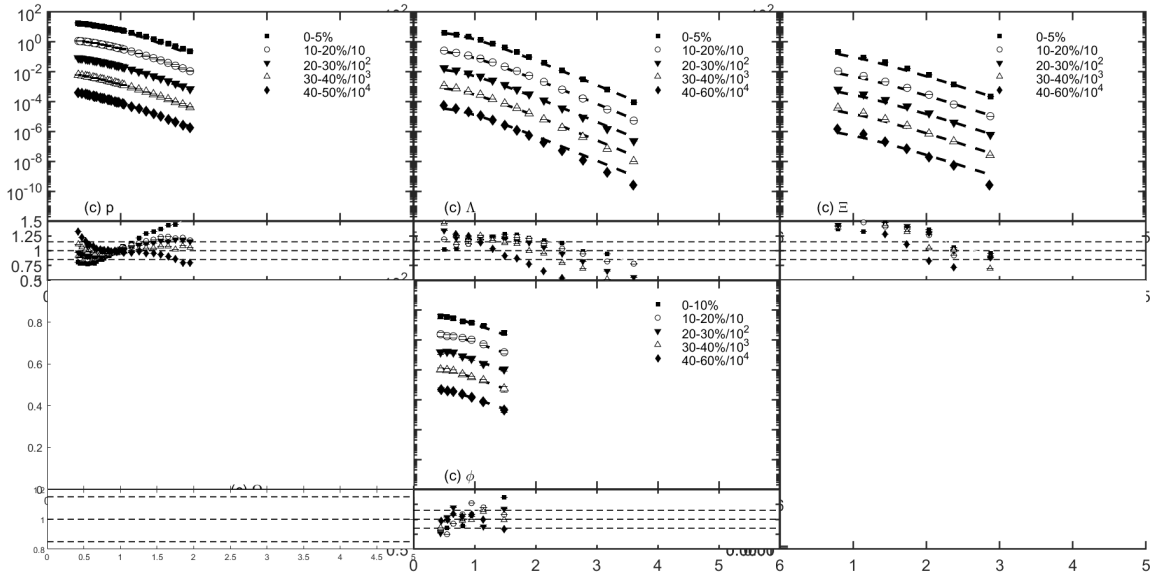

FIG. 9: (colored online)Transverse momentum spectra of proton (a), Λ (b), Ξ (c), Ω (d) and ϕ (e) for Au+Au collisions at $\sqrt{s_{NN}} = 7.7$ GeV and various centralities. The experimental value/theoretical value ratios lie in the bottom of each subfigure. The experimental data are taken from Refs. [1, 7, 8].

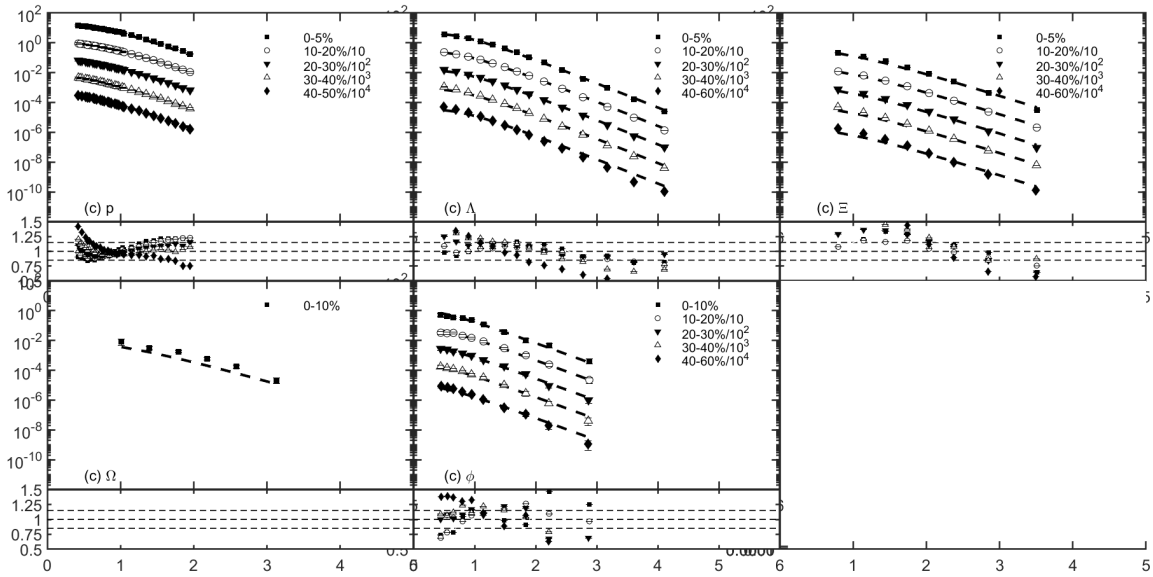

FIG. 10: (colored online)Transverse momentum spectra of proton (a), Λ (b), Ξ (c), Ω (d) and ϕ (e) for Au+Au collisions at $\sqrt{s_{NN}} = 11.5$ GeV and various centralities. The experimental value/theoretical value ratios lie in the bottom of each subfigure. The experimental data are taken from Refs. [1, 7, 8].

collisions is under intensive exploration, it can be expected to improve the theoretical curve to fit data in the future.

With the previous work[3, 4], the successful agreement with available data in the framework of the recombination model indicates that the recombination model work well at such a wide range of $\sqrt{s}$=7.7 GeV∼5.02 TeV. Therefore, we can conclude that the recombination model is one of the optimal approaches to describe the hadronic production in high energy collisions.

Acknowledgements

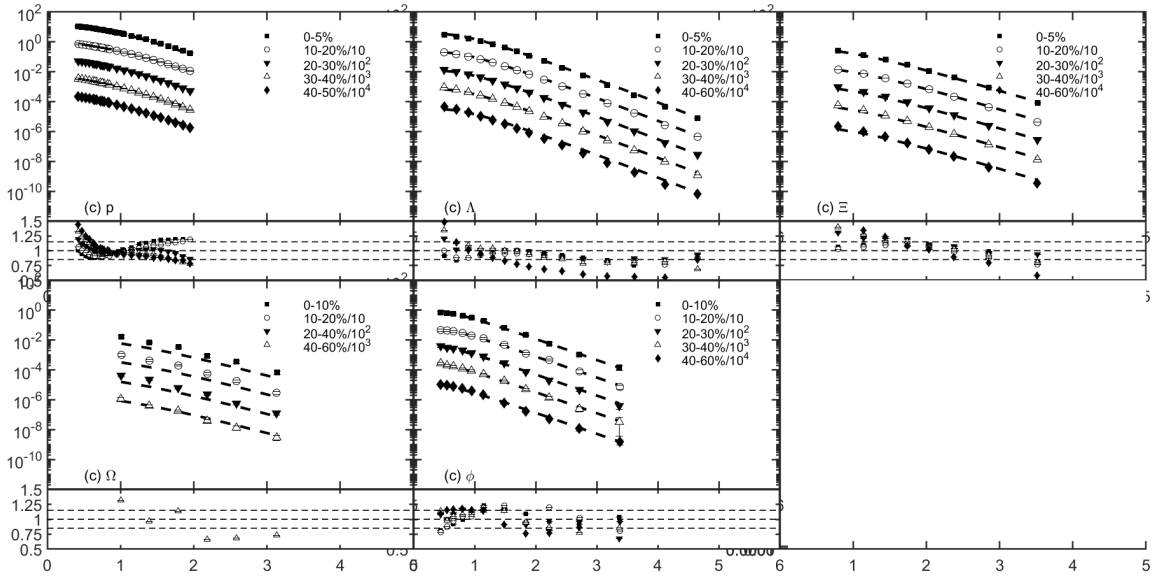

FIG. 11: (colored online)Transverse momentum spectra of proton (a), Λ (b), Ξ (c), Ω (d) and ϕ (e) for Au+Au collisions at $\sqrt{s_{NN}} = 19.6$ GeV and various centralities. The experimental value/theoretical value ratios lie in the bottom of each subfigure. The experimental data are taken from Refs. [1, 7, 8].

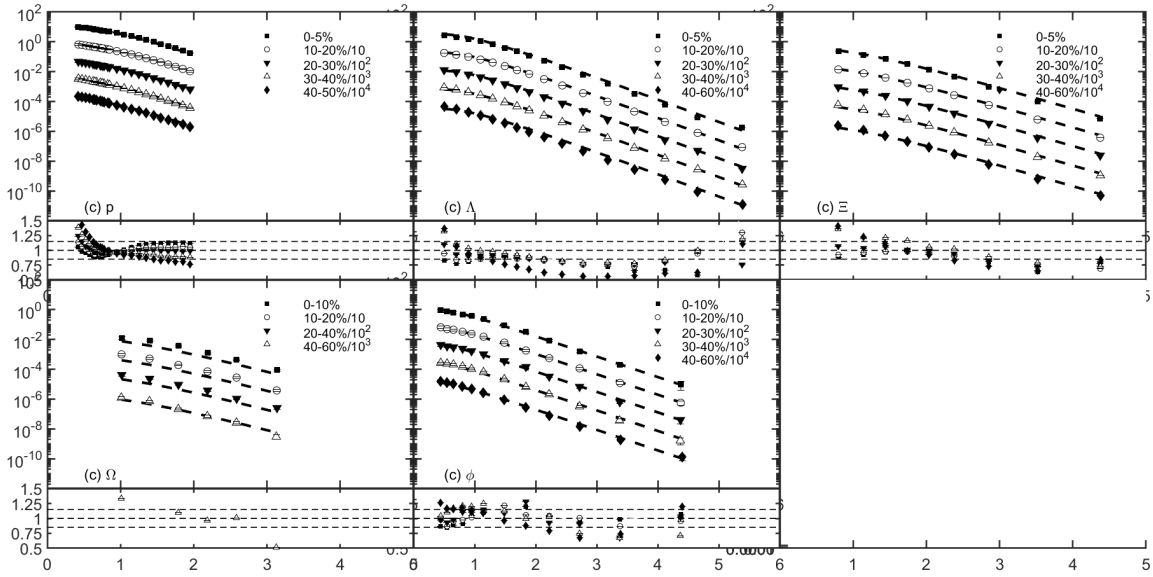

FIG. 12: (colored online)Transverse momentum spectra of proton (a), Λ (b), Ξ (c), Ω (d) and ϕ (e) for Au+Au collisions at $\sqrt{s_{NN}} = 27$ GeV and various centralities. The experimental value/theoretical value ratios lie in the bottom of each subfigure. The experimental data are taken from Refs. [1, 7, 8].

[1] L. Adamczyk *et al.* [STAR], Phys. Rev. C **93**, no.2, 021903 (2016) doi:10.1103/PhysRevC.93.021903 [arXiv:1506.07605 [nucl-ex]].

[2] Lilin Zhu and Rudolph C Hwa 2020 *J. Phys. G: Nucl. Part. Phys.* **47** 055102

[3] Lilin Zhu, Hua Zheng and Rudolph C Hwa 2020, Phys. Rev. C **104**, 014902

[4] Rudolph C Hwa and Lilin Zhu, Phys. Rev. C **97**, 054908 (2018)

[5] R. C. Hwa and C. B. Yang, Phys. Rev. C **66**, 025205(2002)

[6] R. C. Hwa and C. B. Yang, Phys. Rev. C **65**,

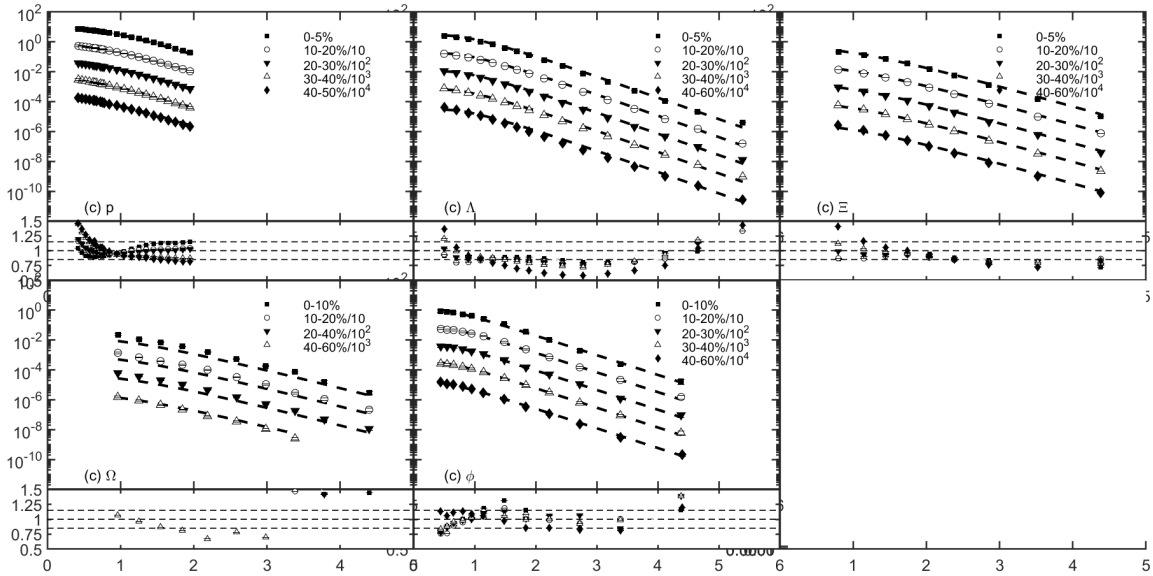

FIG. 13: (colored online)Transverse momentum spectra of proton (a), Λ (b), Ξ (c), Ω (d) and ϕ (e) for Au+Au collisions at $\sqrt{s_{NN}} = 39$ GeV and various centralities. The experimental value/theoretical value ratios lie in the bottom of each subfigure. The experimental data are taken from Refs. [1, 7, 8].

034905 (2002) [erratum: Phys. Rev. C **67**, 059902 (2003)] doi:10.1103/PhysRevC.67.059902 [arXiv:nucl-th/0108043 [nucl-th]].

[7] J. Adam *et al.* [STAR], Phys. Rev. C **102**, no.3, 034909 (2020) doi:10.1103/PhysRevC.102.034909 [arXiv:1906.03732 [nucl-ex]].

[8] L. Adamczyk *et al.* [STAR], Phys. Rev. C **96**, no.4, 044904 (2017) doi:10.1103/PhysRevC.96.044904 [arXiv:1701.07065 [nucl-ex]].

[9] R. C. Hwa and C. B. Yang, Phys. Rev. C **66**, 025204 (2002) doi:10.1103/PhysRevC.66.025204 [arXiv:hep-ph/0202140 [hep-ph]].

[10] L. Zhu and R. C. Hwa, Phys. Rev. C **88**, no.4, 044919 (2013) doi:10.1103/PhysRevC.88.044919 [arXiv:1307.3328 [nucl-th]].

[11] R. C. Hwa and C. B. Yang, Phys. Rev. C **67**, 034902 (2003) doi:10.1103/PhysRevC.67.034902 [arXiv:nucl-th/0211010 [nucl-th]].

[12] R. C. Hwa and C. B. Yang, Phys. Rev. C **70**, 024905 (2004) doi:10.1103/PhysRevC.70.024905 [arXiv:nucl-th/0401001 [nucl-th]].

[13] R. C. Hwa and L. Zhu, Phys. Rev. C **84**, 064914 (2011) doi:10.1103/PhysRevC.84.064914 [arXiv:1109.6300 [nucl-th]].

[14] R. C. Hwa and C. B. Yang, Phys. Rev. C **75**, 054904 (2007) doi:10.1103/PhysRevC.75.054904 [arXiv:nucl-th/0602024 [nucl-th]].

[15] R. C. Hwa and C. B. Yang, Phys. Rev. C **65**, 034905 (2002) [erratum: Phys. Rev. C **67**, 059902 (2003)] doi:10.1103/PhysRevC.67.059902 [arXiv:nucl-th/0108043 [nucl-th]].

[16] R. C. Hwa and M. S. Zahir, Phys. Rev. D **23**, 2539 (1981) doi:10.1103/PhysRevD.23.2539

[17] R. C. Hwa, LA-UR-80-2235.